BeBeC-2018-D2

BAYESIAN SOURCE SEPARATION APPLIED TO ACOUSTIC MEASUREMENTS BY AN ARRAY OF MICROPHONES

Daniel Blacodon[1] and Ali Mohammad-Djafari[2]

[1]Onera – The French Aerospace Lab – F- 92322 Châtillon, France. Daniel.Blacodon@onera.fr

[2]Laboratoire des Signaux et Système, CNRS CentraleSupélec, Université Paris-Saclay, 3, Rue Joliot-Curie, 91192 Gif-sur-Yvette, France. djafari@lss.supelec.fr

ABSTRACT

Active research is ongoing to improve the design of different parts of aircraft including innovative devices of noise reduction often assessed during experiments conducted with scaled models in wind tunnels or in situ with real aircrafts. Source localization methods play a fundamental role to identify the source locations which are at the origin of the annoyance. Another issue for these experiments is the validation of theoretical models, requiring a fine characterization of primary sound sources (source signals). The issue is to extract the primary source signals from the recorded mixtures at the microphone output. Blind signal separation techniques seem to be suitable to respond to this problem.. Bayesian source separation approach has the advantage of incorporating relevant information about sources and mixing systems to help the separation process. It is applied to tests performed in an anechoic chamber with tonal, narrow-band and broadband sources measured with an array of microphones. It is shown that the source separation results are better when sparsity priors are used rather than Gaussian ones for all the sources.

1 INTRODUCTION

The reduction of the flyover noise footprint generated by the aircraft is a priority for the civilian aeronautics industry, which in the next decade will be confronted with more restrictive noise regulation in urban areas. To deal with these issues, active research by engine manufacturers is ongoing in improving the design of inlets [1], fan [2] and compressor blades [3], and nozzles [4], while airframe builders are studying landing gear [5] and flap design [6].

In order to study the efficiency of aircraft noise reduction tools the Computational Aero-Acoustics (CAA) algorithms [7] are frequently used. CAA offers a way to obtain an understanding of the physics at the origin in noise generation by performing numerical

simulations of aeroacoustics phenomena. However, aero-acoustics problems typically involve a broad range of frequencies so that numerical resolution of the high-frequency waves with extremely short wavelengths becomes a great obstacle to accurate numerical simulation with CAA.

It is also possible to use semi-empirical models [8] which are less sophisticated than numerical methods but has a great advantage to provide quick information on the acoustic behaviour of noise sources during development of a new aircraft.

Another important step in understanding the mechanisms at the origin of the noise produced by aircraft concerns the experiments conducted with scaled models in the anechoic wind tunnels or in situ with real aircraft. In these practical situations, source localization methods using sensors arrays [9], [10], [11] often play a fundamental role. Another objective of the experiments is to allow the validation of theoretical models based on knowledge of the original sound sources (source signals) characteristics. In this case, the problem to be solved is different from the source localization, since the issue is to extract the source signals from the recorded mixtures at the sensor output.

Blind Signal Separation (BSS) [12] techniques seem to be suitable to respond to the mentioned problem. The term blind is intended to imply that such methods can separate data into source signal even if very little is known about the nature of those source signals. Independent Component Analysis (ICA) [12] belongs to a class of blind source separation (BSS) methods for separating data into underlying informational components, where such data can take the form of images, sounds, or telecommunication channels.

ICA assumes that the observations are instantaneous linear combinations of the source signals and that the sources are pairwise statistically independent. The mixing matrix is supposed to be invertible which gives the possibility to define a separating matrix.

ICA methods then try to find this separation matrix which will be near to the inverse of the mixing matrix up to a permutation and a scaling ambiguity. Despite success of ICA in separation with simulated signals or in application such as electrocardiogram, image separation, it is problematic when applied to acoustic source separation because the mixing system is not simply instantaneous, but convolutive and sometimes with interferences caused by the reflections of the primary sources. Furthermore, the unobserved source components can be correlated, sparse or positive. This leads naturally to the idea of Informed Source Separation (ISS), where the algorithm design based on Bayesian approach which allows incorporating relevant information about sources and the mixing matrix [13]. This approach is adopted in the present.

In this study, we address Bayesian separation using simulated and experimental data involving three sound sources, which are mixed pairwise on an array of microphones. The first source is monochromatic; the second one has a narrow-band and the third one a broadband. The main objective of this paper is to explore sparse prior distribution to perform the separation of the primary source Power spectral densities based on Bayesian approach with sparsity enforcing priors[14].

The paper is organized as follows. Section 2 introduces briefly the mixtures and the separation models for instantaneous and convolutive applications. Bayesian source separation approach is detailed in Section 3 and in Section 4 Joint Maximum A Posteriori (JMAP) uses for solving the source separation problem. Section 5 presents the experiment carried out with load-speakers, which is used to evaluate the efficiency of the proposed Bayesian source separation method. Section 6 describes tests performed with real observations mixed artificially and their

statistical and spectral analysis. The priors for the mixing matrix, the acoustic sources and the likelihood considered to solve the separation problem are detailed in Section 7. JMAP solutions for the data analysis concerning the experiment described in the paper are presented in Section 8 and in Section 9 the separation solution for the experimental data. These experiment demonstrated that the proposed method is applicable to real world problems of source separation.

2 MIXTURE AND SEPARATION MODELS

The difficulty of the blind source separation task strongly depends on the way in which the signals are mixed within the physical environment. The simplest mixing scenario is termed instantaneous mixing [15], for which most early BSS algorithms were designed. However, real-world acoustical paths lead to convolutive mixing [16] of the sources when measured at the acoustic sensor locations, and the degree of mixing is significant when propagation medium is not anechoic. Both kinds of model are briefly presented in the following.

2.1 Instantaneous Model and ICA

One considers the mixing and filtering processes of the unknown input sources $S_n(t), (n = 1,2, \dots, N)$ that may have different physical models, depending on specific applications. In the simplest case, M mixed signals $x_m(t), (m = 1, 2, \dots, M)$ are assumed to be linear combinations of the N (typically $M \geq N$) unknown source signals $s_n(t)$ [17]:

$$x_m(t) = \sum_{n=1}^{N} a_{m,n} s_n(t) + e_m(t);\ (m = 1,2, \dots, M) \tag{1}$$

or in matrix form:

$$\boldsymbol{x}(\boldsymbol{t}) = \boldsymbol{A}\boldsymbol{s}(\boldsymbol{t}) + \boldsymbol{e}(\boldsymbol{t}) \tag{2}$$

where $\boldsymbol{x}(t) = [x_1(t) \dots x_M(t)]^T$ is a vector of microphone signals, $\boldsymbol{s}(t) = [s_1(t) \dots s_N(t)]^T$ is a vector of sources, $\boldsymbol{e}(t) = [e_1(t) \dots e_M(t)]^T$ is a vector of additive noise, and $\boldsymbol{A}$ is an unknown full rank $M \times N$ mixing matrix containing the coefficients $a_{m,n}, m = 1\ to\ M; n = 1\ to\ N$ of the linear time invariant system characterizing the transfer from the sources to the observations. Thus, it is assumed that the signals received by the array of microphones are weighted sums (linear mixtures) of primary sources.

The objective of blind source separation is to find an inverse system in order to estimate the primary source signals, $\boldsymbol{s}(t)$. This estimation is performed on a vector $\boldsymbol{y}(t) = [y_1(t) \dots y_N(t)]^T$ where $\boldsymbol{y}(t)$ is a linear combinations of the microphone signals $\boldsymbol{x}(t)$. Basically, for linear instantaneous mixtures, ICA methods aim at estimating a demixing matrix $\boldsymbol{B}$ yielding estimated sources $\boldsymbol{y}(t) = [y_1(t) \dots y_N(t)]^T$ (Fig.1).

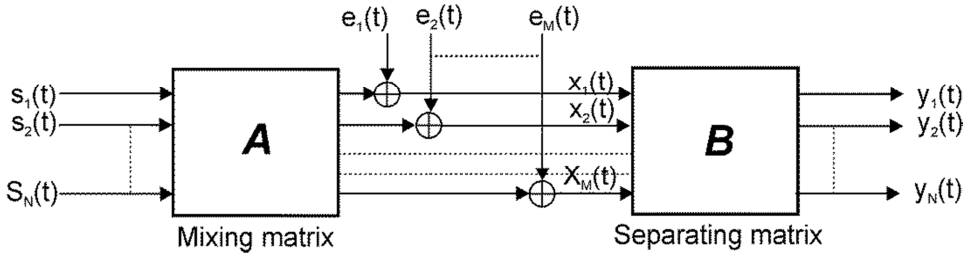

Fig.1. Block diagram of the instantaneous BSS task.

The majority of research efforts for estimating $\boldsymbol{B}$ have been devoted to the noiseless case, where $\boldsymbol{e}(t) = \boldsymbol{0}$. Thus, it is not too difficult to show, if $\boldsymbol{A}$ is inversible $\widehat{\boldsymbol{B}} = \boldsymbol{A}^{-1}$, then $\boldsymbol{y}(t) = \widehat{\boldsymbol{B}}\boldsymbol{x}(t) = \widehat{\boldsymbol{B}}\boldsymbol{A}\boldsymbol{s}(t) = \boldsymbol{s}(t)$. The output independence for $\boldsymbol{y}(t)$ leads to a matrix $\boldsymbol{B}$ that satisfies $\boldsymbol{B}\boldsymbol{A} = \boldsymbol{P}\boldsymbol{D}$, where $\boldsymbol{P}$ is a permutation matrix and $\boldsymbol{D}$ a scale matrix [17]. The estimated $\boldsymbol{y}(t)$ are equal to the primary sources $\boldsymbol{s}(t)$, up to a permutation and a scale. A convenient criterion of independence is the Kullback-Leibler KL divergence [18]:

$$KL\left(p_y(\boldsymbol{y}), \prod_{n=1}^{N} p_{y_n}(y_n)\right) = \int_{\mathbb{R}^N} p_y(\boldsymbol{y}) log\left(\frac{p_y(\boldsymbol{y})}{\prod_{n=1}^{N} p_{y_n}(y_n)}\right) d\boldsymbol{y} \tag{3}$$

The divergence KL has the property to be null only when the variables $\{y_n\}_{n=1}^{N}$ are statistically independent. This allows obtaining an estimate for $\boldsymbol{B}$ as follows:

$$\hat{B} = arg \max_{\boldsymbol{B}} KL\left[\left(p_y(\boldsymbol{y}), \prod_{n=1}^{N} p_{y_n}(y_n)\right)\right] \tag{4}$$

The estimation of a separating matrix $\boldsymbol{B}$ in the presence of noise is rather difficult. The effect of incident noise fields impinging on M microphones may be considered to be equivalent to additional sources, and thus are subject to the same separation process as the desired N source signals. It is obvious, that we are not interested in separation of source noises, and their cancellation is a major issue to solve. At this point, it is worth mentioning that ICA methods allow only to obtain an unbiased estimate of the unmixing matrix $\widehat{\boldsymbol{B}}$. Furthermore, due to memoryless structure of such methods, by definition, they cannot remove the additive noise. Therefore, the vector representing independent components can be written as:

$$\boldsymbol{y}(t) = \widehat{\boldsymbol{B}}\boldsymbol{x}(t) = \widehat{\boldsymbol{B}}\big(\boldsymbol{A}\boldsymbol{s}(t) + \boldsymbol{e}(t)\big) = \widehat{\boldsymbol{y}}(t) + \tilde{\boldsymbol{e}}(t) \tag{5}$$

where $\widehat{\boldsymbol{y}}(t) = \widehat{\boldsymbol{B}}\boldsymbol{A}\boldsymbol{s}(t)$ is the vector of noise free independent signals and $\tilde{\boldsymbol{e}}(t) = \widehat{\boldsymbol{B}}\boldsymbol{e}(t)$ denotes the noise component.

2.2 Convolutive model in time domain and ICA

While many algorithms have been developed for instantaneous mixing models, in many real-world applications, such as acoustic tests carried out in a closed jet wind tunnel, without any acoustic liner installed on the walls of the test section, the mixing process is more

complex. In such situation, convolutive mixing arises due to time delays resulting from sound propagation over space and the multipath generated by reflections on the reflective surfaces of the test section.

Consider here that N sources $\boldsymbol{s_v}(t) = [s_{v_1}(t) \dots s_{v_N}(t)]^T$ radiate from locations $\boldsymbol{v} = [v_{1\dots}v_N]$ on M microphones at positions $\boldsymbol{r(t)} = [r_1(t) \dots r_N(t)]$. The observations $x(r_m, t)$ measured by the m^{th} microphone, concerning the original sources are generally done in practical situations with background noise. Therefore, $x(r_m, t)$ can be modelled as follows:

$$x(r_m, t) = \sum_{n=1}^{N} \int_{0}^{+\infty} a_{r_m, v_n} s_{v_n}(t-\tau) d\tau + e_m(t) \tag{6}$$

where a_{r_m,v_n} are coefficients at time t of the mixing matrix $a_{\boldsymbol{r},\boldsymbol{v}}$, characterizing the impulse response of the propagation medium between the original sources and the microphones. Hereafter, in order to simplified the notations, $x(r_m, t)$, a_{r_m,v_n} and s_{v_n} are replaced with $x_m(t)$, $a_{m,n}$, $s_n(t)$ respectively.

We assume now, that the impulse responses can be modelled by a finite impulse response (FIR) of length L and the observations sampled at frequency f_s. In this case, $x_m(t)$ measured at the discrete time $t_k = {}^{k}/_{f_s}$ takes the form:

$$x_m(k) = \sum_{n=1}^{N} \sum_{l=1}^{L} a_{m,n,l} s_n(k-l) + e_m(k) \tag{7}$$

where $a_{m,n} = (a_{m,n,0}, \dots, a_{m,n,L})$.

Eq.(7) models the acoustic mixing as a multiple-input multiple-output (MIMO) linear system (Fig.2).

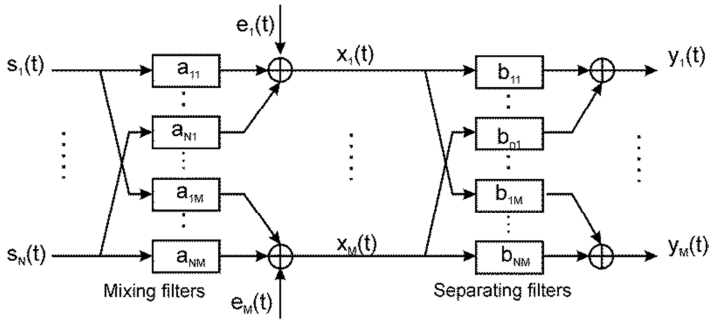

Fig.2. Block diagram of the convolutive BSS task.

As for the instantaneous separation problem (see Sect. (Instantaneous Model and ICA)), the aim of multichannel deconvolution is to recover the source signals $\boldsymbol{s}(k)$ from the observations $\boldsymbol{x}(k)$, up to a scaled, permuted, and delayed version of source signals, i.e., the estimates of sources $\boldsymbol{y}(k) = \hat{\boldsymbol{s}}(k) = \boldsymbol{PD}(k)\boldsymbol{s}(k)$ This is usually achieved by estimating a matrix of unmixing filters $b_{m,n} = (b_{m,n,0}, \dots, b_{m,n,L})$ giving for the n[th] source signal:

$$y_n(k) = \sum_{l=0}^{L} \sum_{m=1}^{M} b_{m,n,l} x_n(k-l)\ ;\ \ n = 1, \dots N \tag{8}$$

It is possible to write $y_n(k)$ in terms of the source signals by substituting $x_m(k)$ Eq.(7) into Eq.(8):

$$y_n(k) = \hat{y}_{s,n} + y_{IPS,n} + y_{BN,n} \tag{9}$$

where:

$$\hat{y}_{s,n}(k) = \sum_{m=1}^{M} (b_{mn} * a_{mn} * s_n)(k) \tag{10}$$

contains the desired primary source $s_n(k)$ and where $*$ denotes the convolution operator;

$$y_{IPS,n}(k) = \sum_{\substack{n'=1 \\ n' \neq n}}^{N} \ \sum_{m=1}^{M} (b_{mn'} * a_{mn'} * s_n)(k) \tag{11}$$

is Interfering Point Sources IPS;

$$y_{BN,n}(k) = \sum_{m=1}^{M} (b_{mn} * e_m)(k) \tag{12}$$

denotes the Background Noise component.

Eq.(9) shows that in the case of noisy convolutive mixtures, the separation filters $b_{m,n}$ must remove the both the interference introduced by the mixing process and the noise component. In general, BSS algorithms focus on the suppression of interfering point sources and have only a limited capability of attenuating background noise.

2.3 Convolutive model in frequency domain

Time-domain algorithms can be developed to perform the separation task. However, they can be difficult to code primarily due to the multichannel convolution operations involved. One way to simplify the conceptualization of convolutive BSS algorithms is to transform the separation problem into the frequency domain. The linear convolution in the time domain (Eq.(7)) can be written in the frequency domain as separate multiplications for each frequency:

$$\boldsymbol{X}(\omega) = \boldsymbol{A}(\omega)\boldsymbol{S}(\omega) + \boldsymbol{E}(\omega) \tag{13}$$

At each frequency $\omega = 2\pi f$, $\boldsymbol{A}(\omega)$ is a complex $M \times N$ matrix, $\boldsymbol{X}(\omega)$ and $\boldsymbol{E}(\omega)$ are complex $M \times 1$ vector and similarly $\boldsymbol{S}(\omega)$ is a $N \times 1$ vector. The frequency transformation is typically computed using a Discrete Fourier Transform (DFT) of $\boldsymbol{x}(t)$, $\boldsymbol{e}(t)$, $\boldsymbol{s}(t)$, within a time frame of prescribed length. It is clear that the convolutive mixtures blind separation in a time-domain is changed into instantaneous mixtures blind separation in the frequency-domain. Therefore, instantaneous mixtures blind separation methods in the frequency domain can be used to solve the blind deconvolution problems in the time domain.

Each frequency component of the mixture signal contains an instantaneous mixture of the corresponding frequency components of the underlying source signals. The separation operation at the frequency consists in finding $\boldsymbol{B}(\omega)$ such that:

$$\boldsymbol{Y}(\omega) = \boldsymbol{B}(\omega)\boldsymbol{X}(\omega) \tag{14}$$

and by taking into account (Eq.(13)), we have:

$$\boldsymbol{Y}(\omega) = \boldsymbol{B}(\omega)\boldsymbol{A}(\omega)\boldsymbol{S}(\omega) + \boldsymbol{B}(\omega)\boldsymbol{E}(\omega) \tag{15}$$

An accurate separation will be occurred if:

$$\boldsymbol{B}(\omega)\boldsymbol{A}(\omega) = \boldsymbol{I} \tag{16}$$

and the background noise $\boldsymbol{E}(\omega)$ removed before the separation process.

3 BAYESIAN SOURCE SEPARATION

The problem of source separation is particularly difficult to solve when it concerns acoustic sources. One of the ways to facilitate separation, is to take into account any information previously available on the source signals and the mixing coefficients [18]. Bayesian methods are quite suitable for this task, since they naturally integrate information. Moreover, there is a remarkable aspect of Bayesian source separation methods which is their robustness to noise. Indeed, differently from ICA methods, the Bayesian approach takes noise into account in its formulation [14].

3.1 Formulation

The problem is formulated in a probabilistic framework by treating the mixture matrix, sources and observations as random variables. The fundamental point in the Bayesian approach is Baye's theorem which allows to merge all those information in order to deduce a posterior probability description of the unknown variables:

$$p(\boldsymbol{A}, \boldsymbol{S}|X) \propto p(X|\boldsymbol{A}, \boldsymbol{S})p(\boldsymbol{A})p(\boldsymbol{S}) \tag{17}$$

where $p(\boldsymbol{A}, \boldsymbol{S}|\boldsymbol{X})$ is the joint posterior probability density of the unknown $\boldsymbol{A}$ and $\boldsymbol{S}$, $p(\boldsymbol{X}|\boldsymbol{A}, \boldsymbol{S})$ is the likelihood and $p(\boldsymbol{A})$ and $p(\boldsymbol{S})$ the prior probability densities.

Let us denote by $\boldsymbol{\theta} = (\boldsymbol{\theta}_A, \boldsymbol{\theta}_S, \boldsymbol{\theta}_E)$ the set of the hyperparameters associated respectively with the variables $\boldsymbol{A}$ and $\boldsymbol{S}$ and $\boldsymbol{E}$ of the mixing model (Eq.(7)). Then we have:

$$p(\boldsymbol{A},\boldsymbol{S}|\boldsymbol{X},\boldsymbol{\theta}) \propto p(\boldsymbol{X}|\boldsymbol{A},\boldsymbol{S},\boldsymbol{\theta}_E)p(\boldsymbol{A},\boldsymbol{\theta}_A)p(\boldsymbol{S},\boldsymbol{\theta}_S) \tag{18}$$

This relation is the point of the Bayesian source separation using $p(\boldsymbol{A},\boldsymbol{S}|\boldsymbol{X},\boldsymbol{\theta})$. Different estimators for $\boldsymbol{A}$ and $\boldsymbol{S}$ can be defined. One of them considered in this study is the Joint Maximum A Posterior (JMAP).

4 JOINT MAXIMUM A POSTERIORI (JMAP) ESTIMATION

The JMAP estimator is defined as:

$$(\widehat{\boldsymbol{A}},\widehat{\boldsymbol{S}}) = arg\max_{(\boldsymbol{A},\boldsymbol{S})}\{p(\boldsymbol{A},\boldsymbol{S}|\boldsymbol{X},\boldsymbol{\theta})\} = \operatorname{argmin}_{(\boldsymbol{A},\boldsymbol{S})}\{J(\boldsymbol{A},\boldsymbol{S})\} \tag{19}$$

where:

$$\begin{aligned} J(\boldsymbol{A},\boldsymbol{S}) &= -ln\{p(\boldsymbol{A},\boldsymbol{S}|\boldsymbol{X},\boldsymbol{\theta})\} \\ &= \boldsymbol{Q}_1 + \boldsymbol{Q}_2 + \boldsymbol{Q}_3 \end{aligned} \tag{20}$$

$$\begin{cases} \boldsymbol{Q}_1 = -\ln\big(p(\boldsymbol{X}|\boldsymbol{A},\boldsymbol{S},\boldsymbol{\theta}_E)\big) \\ \boldsymbol{Q}_2 = -\ln\big(p(\boldsymbol{A}|\boldsymbol{\theta}_A)\big) \\ \boldsymbol{Q}_3 = -\ln\big(p(\boldsymbol{S}|\boldsymbol{\theta}_S)\big) \end{cases} \tag{21}$$

The first term $\boldsymbol{Q}_1$ of the criterion represents the ad-equation to the observations which is obtained from the likelihood, while the two last terms $\boldsymbol{Q}_2$ and $\boldsymbol{Q}_3$ of the criterion depend only on the priors $p(\boldsymbol{A})$ and $p(\boldsymbol{S})$. One of the easiest optimization methods for $J(\boldsymbol{A},\boldsymbol{S})$ is an alternate optimization with respect to $\boldsymbol{A}$ and then to $\boldsymbol{S}$ [19]:

$$\begin{cases} \widehat{\boldsymbol{A}} = \operatorname{argmin}_{\boldsymbol{A}}\big\{J(\boldsymbol{A},\widehat{\boldsymbol{S}})\big\} \\ \widehat{\boldsymbol{S}} = \operatorname{argmin}_{\boldsymbol{A}}\big\{J(\widehat{\boldsymbol{A}},\boldsymbol{S})\big\} \end{cases} \tag{22}$$

Studying the convergence properties of such algorithms in general is not easy. There is no guarantee that such algorithms converge toward the global JMAP solutions, but may converge to any local minimum. However, satisfactory solutions can be obtained by choosing appropriate priors $p(\boldsymbol{A})$ and $p(\boldsymbol{S})$ or by imposing constraints on the mixing matrix and on the sources [12].

5 EXPERIMENT WITH LOUDSPEAKERS

In the framework of this study an experiment has been carried out in anechoic room to evaluate the ability of Bayesian source separation method to separate successfully acoustic sources that simulate practical situations (Fig.3). The acoustic sources are radiated by three load-speakers $LS1$, $LS2$, and $LS3$. $LS1$ radiates a pure sine source S_1 at 4 kHz. $LS2$ emits a narrow band source S_2 in the frequency range [3 kHz, 5 kHz] and $LS3$ a broadband source S_3 in the range [2 kHz, 10 kHz]. The acoustic radiation of the sources is measured by an array of

fifteen microphones. Three reference microphones Ref_1, Ref_2 and Ref_3 where also mounted, near the output of the load-speakers. The acoustic waves $s_1(t)$, $s_2(t)$ and $s_3(t)$ emitted respectively by $LS1$, $LS2$, and $LS3$ were individually measured both by the array of microphones and reference microphones.

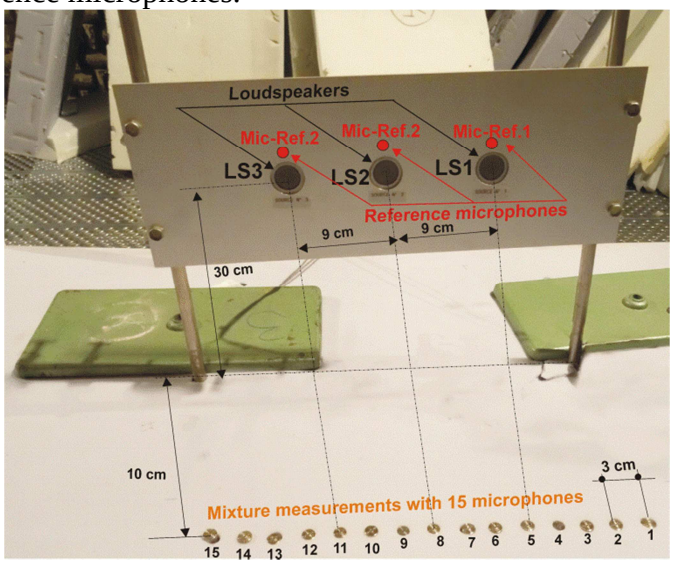

Fig. 3. Experimental set-up in an anechoic chamber.

The measurements by the array were also performed when the couples of load-speakers ($LS1$, $LS2$), ($LS1$, $LS3$), and ($LS2$, $LS3$), were active to produce on the microphones the signal mixtures $s_{12}(t) = s_1(t) + s_2(t)$, $s_{13}(t) = s_1(t) + s_3(t)$, $s_{23}(t) = s_2(t) + s_3(t)$. The objective followed in this study is to separate the power spectral densities (PSD) of S_1 , S_2 and S_3 from the PSDs of the mixtures $s_{12}(t)$, $s_{13}(t)$ and $s_{23}(t)$. In order to simplify the reading of the article the following notations are adopted; 1) S_i ($i = 1\ to\ 3$) is associated to both to source number j and to its PSD S_j ; 2) ($S_i + S_j$) represents the PSD of the mixture $s_{ij}(t) = s_i(t) + s_j(t)$ ($i,\ j\ =\ 1\ \ to\ 3\ and\ i\ \neq\ j$) measured by the array.

Clearly, situation is arduous because the supports in the frequency domain of the three primary sources overlap. The source separation based on a Bayesian approach takes on its full meaning since prior information on the primary sources can be exploited to help their separation. Indeed, we have $\boldsymbol{S}_1$ and $\boldsymbol{S}_2$ which radiate in a frequency band munch weaker than $\boldsymbol{S}_3$, and $\boldsymbol{S}_1$ in a frequency band munch weaker than $\boldsymbol{S}_2$. This naturally will lead to use of parsimony in the frequency domain to facilitate the source separation considered hereafter.

6 TESTS WITH ARTIFICIAL MIXTURES

Before preceding the source separation starting from the measured signals with the microphone array, trials of source separation were performed with artificial mixtures of the real sources. In a first step, the signals measured at the output of the reference microphones ef_1 , Ref_2 and Ref_3 were filtered in frequency bands [3.8 kHz, 4.2 kHz], [1 kHz, 8 kHz] and [0.3 kHz, 14 kHz] respectively. The results of the filtering constitute the primary source signals S_1, S_2 and S_3 . These later were numerically mixed pairwise according to the convolutive model described by (Eq.(7)). The mixing coefficients have been chosen to obtain

the same PSDs levels as those measured on the microphones during the experiment presented in Section 5. Thus, the pressure field $x_i(t)$ received on the i^{th} microphone is of the form:

$$x_i(t) = \begin{pmatrix} a_{ik} & 0 \\ 0 & a_{il} \end{pmatrix} \begin{pmatrix} s_k(t) \\ s_l(t) \end{pmatrix} + e_i(t) \tag{23}$$

where the subscripts for the mixing coefficients of $\boldsymbol{A}$ and $\boldsymbol{S}$ stand for:

$$\begin{cases} k,l = 1,2 \; when \; S_1 \; and \; S_2 \; are \; active \\ k,l = 1,3 \; when \; S_1 \; and \; S_3 \; are \; active \\ k,l = 2,3 \; when \; S_2 \; and \; S_3 \; are \; active \end{cases} \tag{24}$$

It should be noted that, although artificial, the mixed signals thus obtained correspond of mixture actually encountered in the experimental setup defined in Section 5.

6.1 Artificial mixtures analysis

The upper plots in Fig.4 show the time series of $\boldsymbol{S}_1$ the sine at 4 kHz, $\boldsymbol{S}_2$, the narrow band source in the range [3 kHz, 5 kHz] and $\boldsymbol{S_3}$ the broadband source in the interval [2 kHz, 10 kHz]. The plots in the centre present the histogram of S_1 where two regions are dominant, corresponding to high and lower levels of the $\boldsymbol{S}_1$. Nevertheless, the histograms of $\boldsymbol{S}_2$ and $\boldsymbol{S}_3$, exhibit a bell shape (center graphs) corresponding to a Gaussian distribution. Scatter displayed in the lower plots depict joint distributions of the primary sources (lower graphs). It appears that; i) $\boldsymbol{S_1}$ and $\boldsymbol{S}_2$ are independent with uniform distributions on a parallelogram; ii) the same comments can be done for $\boldsymbol{S}_1$ and $\boldsymbol{S}_3$; iii) the scatter plot for $\boldsymbol{S_2}$ and $\boldsymbol{S}_3$ shows this time a distribution of two independent Gaussian signals which is rotationally symmetrical.

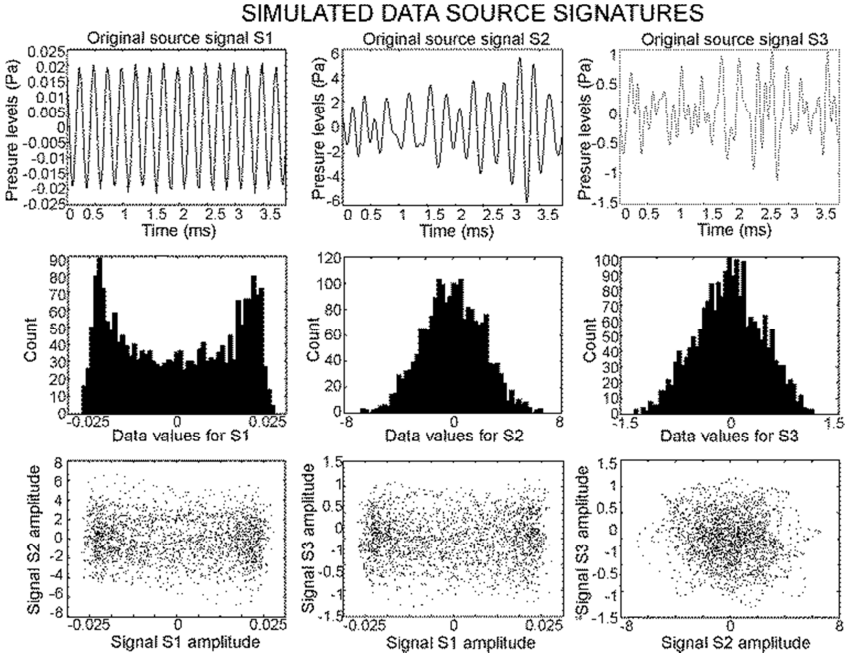

Fig. 4. Primary source signals $\boldsymbol{S}_1$, $\boldsymbol{S}_2$ and $\boldsymbol{S}_3$ (upper) - Histograms of the primary source signals (centre) - Joint distributions of the primary source signals (lower).

The upper graphs in Fig.5 exhibits the Power Spectral Densities (PSD) of the primary source signals shown in Fig.4 (upper graphs). In the center of Fig.5, it is superimposed from left to right the PSDs of ($\boldsymbol{S}_1$, $\boldsymbol{S}_2$), ($\boldsymbol{S}_1$, $\boldsymbol{S}_3$) and ($\boldsymbol{S}_2$, $\boldsymbol{S}_3$) measured with the virtual microphone number one of the array. The mixtures of the PSDs ($\boldsymbol{S}_1$ + $\boldsymbol{S}_2$), ($\boldsymbol{S}_1$ + $\boldsymbol{S}_3$) and ($\boldsymbol{S}_2$ + $\boldsymbol{S}_3$) on which will be applied the Bayesian separation of sources are presented in the lower plots.

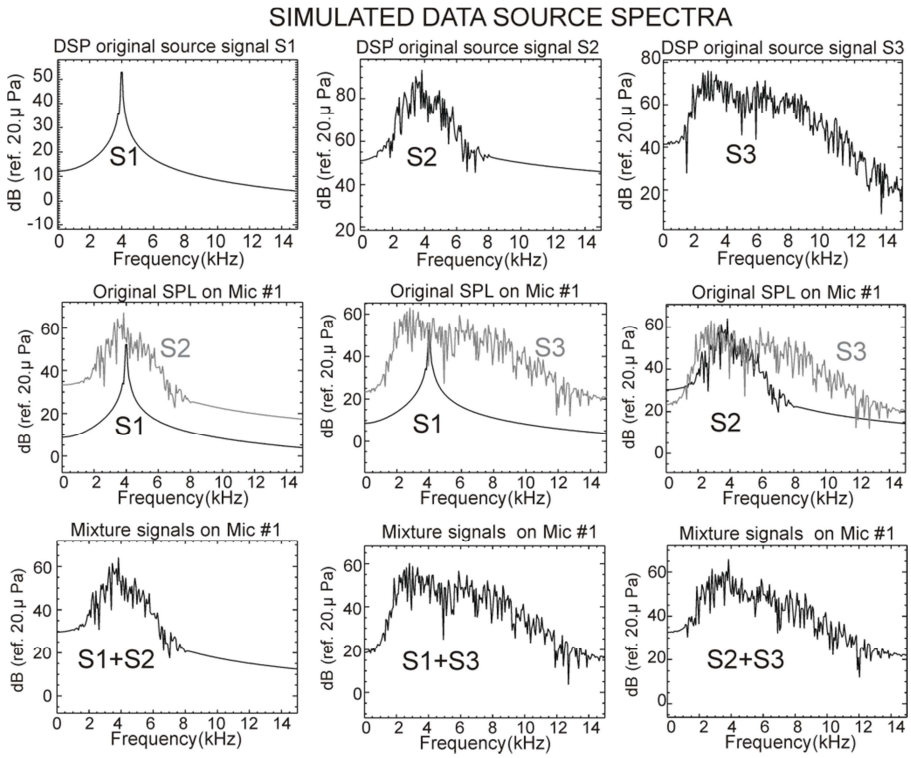

Fig.5. PSDs of primary source signals shown in the upper plots of Fig.4 (upper) - Superposition of source signal PSDs ($\boldsymbol{S}_1$, $\boldsymbol{S}_2$), ($\boldsymbol{S}_1$, $\boldsymbol{S}_3$) and ($\boldsymbol{S}_2$, $\boldsymbol{S}_3$) (centre) - Artificial mixtures of primary sources (lower)

7 SOURCE AND MIXING MATRIX PRIOR CHOICE – LIKELIHOOD DESCRIPTION

It is necessary to defined the priors $p(\boldsymbol{A})$, $p(\boldsymbol{S})$ and the likelihood $p(\boldsymbol{X}|\boldsymbol{A},\boldsymbol{S})$ allowing to defined the posterior probability Eq.(17) for solving the Bayesian source separation problem defined by Eq.(19) for the data obtained from the experiment described in Sections 5 and 6 when the acoustic sources are pairwise active.

7.1 Source priors

We have different possible priors for acoustic sources $\boldsymbol{S}_1$, $\boldsymbol{S}_2$ and $\boldsymbol{S}_3$, depending on many design choices, and each combination of these choices giving a different algorithm. We define three cases in order to assess the separation capability.

7.1.1 Gaussian priors for $\boldsymbol{S}$

In this first case, we consider that there is no specific knowledge on the three acoustic sources. In order to represent our state of ignorance, we can adopt for $\boldsymbol{S}_1$, $\boldsymbol{S}_2$ and $\boldsymbol{S}_3$ to have as prior law, a Gaussian distribution, with zero-mean, and of dispersion law $\sigma_{S_i}^2$ (i=1 to 3), thus:

$$S_i \sim \mathcal{N}\left(\boldsymbol{S}_i | 0, \sigma_{S_i}^2\right) \propto exp\left\{-\frac{1}{2\sigma_{S_i}^2}\|\boldsymbol{S}_i\|_2^2\right\} \tag{25}$$

7.1.2 Sparsity prior for $\boldsymbol{S}_1$ and Gaussian priors for $\boldsymbol{S}_2$ and $\boldsymbol{S}_3$

This second case considers that $\boldsymbol{S}_1$ is mixed either with $\boldsymbol{S}_2$ or $\boldsymbol{S}_3$ It is assumed to be known that the acoustic radiation of $\boldsymbol{S}_1$ is performed in a weaker frequency band than $\boldsymbol{S}_2$ or $\boldsymbol{S}_3$. The spectrum of $\boldsymbol{S}_1$ can then be considered sparse (i.e. has only few nonzero elements) in the frequency domain. This information can be translated via Laplace density:

$$S_1 \sim \mathcal{L}(\boldsymbol{S}_1 | \alpha_1) \propto exp\{-\alpha_1 \|\boldsymbol{S}_1\|_1\} \tag{26}$$

7.2 Mixing matrix prior

The elements of the mixing matrix $\boldsymbol{A}$ reflect the coupling between the sources and microphones. In a clearly physical situation, these matrix elements depend on the physical transmission from the sources to the microphones. For now, we consider the situation where the mixing process is modelled generically because it is not well understood. Indeed, in the experiment described in Section 5, the sources are very close to the microphones. Thus, the attenuation of the source levels, between their emission locations, to the microphones, does not follow the classical geometric law in 1/R (R is the distance between the sources and the microphones). In order to represent our state of ignorance on $\boldsymbol{A}$, it is assumed that the mixing matrix has a Gaussian distribution of zero-mean and with a diagonal covariance matrix σ_A^2:

$$\boldsymbol{A} \sim \mathcal{N}(\boldsymbol{A} | 0, \sigma_A^2) \propto exp\left\{-\frac{1}{2\sigma_A^2}\|\boldsymbol{A}\|_2^2\right\} \tag{27}$$

7.3 Likelihood

It is assumed that the noise associated with the experimental measurements can reasonably be represented as a centered Gaussian process:

$$\boldsymbol{E} \sim \mathcal{N}(\boldsymbol{E} | 0, \sigma_E^2) \propto exp\left\{-\frac{1}{2\sigma_E^2}\|\boldsymbol{E}\|_2^2\right\} \tag{28}$$

The covariance of the noise indicates that each component of $\boldsymbol{E}$ in Eq.(7) is contaminated by independent identically distributed random noise. The likelihood can be therefore written of the form:

$$p(\boldsymbol{X} | \boldsymbol{A}, \boldsymbol{S}, \boldsymbol{\theta}_E) \propto exp\left\{-\frac{1}{2\sigma_E^2}\|\boldsymbol{X} - \boldsymbol{A}\boldsymbol{S}\|_2^2\right\} \tag{29}$$

8 JMAP SOLUTIONS FOR THE DATA ANALYSIS

We have described in Section 4 the principle of the optimization method for obtaining generic JMAP solutions $\boldsymbol{A}$ and $\boldsymbol{S}$. In the following we examine the possible solutions which can be obtained for the mixing cases defined with Eq.(24), by using Eq.(27) for the matrix prior, Eq.(28) for the likelihood and Eqs.(25) and (26) depending the source priors considered.

8.1 JMAP : Gaussian priors $\boldsymbol{S}$

In this first situation, we consider that the three acoustic sources $\boldsymbol{S}_1$, $\boldsymbol{S}_2$ and $\boldsymbol{S}_3$ have Gaussian priors, defined by Eq.(25). By taking into account the Eqs.(27) and (28), the logarithm of the joint density Eq.(20), becomes:

$$J(\boldsymbol{A},\boldsymbol{S}) = \frac{1}{2\sigma_E^2}\|\boldsymbol{X} - \boldsymbol{A}_k\boldsymbol{S}_k - \boldsymbol{A}_l\boldsymbol{S}_l\|_2^2 + \frac{1}{2\sigma_A^2}\|\boldsymbol{A}\|_2^2 + \frac{1}{2\sigma_{S_k}^2}\|\boldsymbol{S}_k\|_2^2 + \frac{1}{2\sigma_{S_l}^2}\|\boldsymbol{S}_l\|_2^2 \tag{30}$$

During the iterative process, analytic solutions are used to compute estimates of $\boldsymbol{A}$ (where $\boldsymbol{S}_k$ and $\boldsymbol{S}_l$ are assumed to be known) of $\boldsymbol{S}_k$ (where $\boldsymbol{A}$ and $\boldsymbol{S}_l$ are assumed to be known) and of $\boldsymbol{S}_l$ (where $\boldsymbol{A}$ and $\boldsymbol{S}_k$ are assumed to be known):

$$\begin{cases} \hat{A}^i = X\hat{S}^T\left(\hat{S}\hat{S}^t + \lambda_A I\right)^{-1} \\ \widehat{S}_k^i = \left(\hat{A}_k^t\hat{A}_k + \lambda_{S_k} I\right)^{-1}(\hat{A}_k^t X - \hat{A}_l^t\hat{A}_k\hat{S}_l) \\ \hat{S}_l^i = \left(\hat{A}_l^t\hat{A}_l + \lambda_{S_l} I\right)^{-1}(\hat{A}_l^t X - \hat{A}_k^t\hat{A}k_l\hat{S}_k) \end{cases} \tag{31}$$

where:

$$\begin{cases} \lambda_A = \dfrac{\sigma_E^2}{\sigma_A^2} \\ \lambda_{S_k} = \dfrac{\sigma_E^2}{\sigma_{S_k}^2} \\ \lambda_{S_l} = \dfrac{\sigma_E^2}{\sigma_{S_l}^2} \end{cases} \tag{32}$$

8.2 JMAP SPARSE : Sparsity prior for $\boldsymbol{S}_1$ and Gaussian priors $\boldsymbol{S}_2$ and $\boldsymbol{S}_3$

For the third case corresponding to the mixing of $\boldsymbol{S}_1$ with $\boldsymbol{S}_2$ or $\boldsymbol{S}_3$. $\boldsymbol{S}_1$ has a Laplace prior Eq.(26) to take into account the sparsity of its PSD. $\boldsymbol{S}_2$ and $\boldsymbol{S}_3$ has a Gaussian prior Eq.(25). By taking into account the Eqs.(27) and (28), the logarithm of the joint density Eq.(20), becomes:

$$J(\boldsymbol{A},\boldsymbol{S}) = \frac{1}{2\sigma_E^2}\|\boldsymbol{X} - \boldsymbol{A}_k\boldsymbol{S}_k - \boldsymbol{A}_1\boldsymbol{S}_1\|_2^2 + \frac{1}{2\sigma_A^2}\|\boldsymbol{A}\|_2^2 + \frac{1}{2\sigma_{S_k}^2}\|\boldsymbol{S}_k\|_2^2 + \alpha_1\|\boldsymbol{S}_1\|_1 \tag{33}$$

where the subscript $k = 2$ or $k = 3$ are used when $\boldsymbol{S}_2$ or $\boldsymbol{S}_3$ is respectively active.

According to Eq.(22)), the estimates of $\boldsymbol{A}$ and $\boldsymbol{S}$ can be obtained using a three steps algorithm ALS [19]:

$$\begin{cases} \hat{A}^i = \underset{\boldsymbol{A}}{\text{argmin}} & \{\|\boldsymbol{X} - \boldsymbol{A}_k\boldsymbol{S}_k - \boldsymbol{A}_1\boldsymbol{S}_1\|_2^2 + \lambda_A\|\boldsymbol{A}\|_2^2\} \\ \widehat{S}_k^i = \underset{S_k}{\text{argmin}} & \{\|\boldsymbol{X} - \boldsymbol{A}_k\boldsymbol{S}_k - \boldsymbol{A}_1\boldsymbol{S}_1\|_2^2 + \lambda_{S_K}\|\boldsymbol{S}_k\|_2^2\} \\ \hat{S}_1^i = \underset{S_1}{arg\min} & \{\|\boldsymbol{X} - \boldsymbol{A}_k\boldsymbol{S}_k - \boldsymbol{A}_1\boldsymbol{S}_1\|_2^2 + \lambda_1\|\boldsymbol{S}_1\|_1\} \end{cases} \tag{34}$$

where:

$$\begin{cases} \lambda_A = \dfrac{\sigma_E^2}{\sigma_A^2} \\ \lambda_{S_k} = \dfrac{\sigma_E^2}{\sigma_{S_k}^2} \\ \lambda_1 = \alpha_1\sigma_E^2 \end{cases} \tag{35}$$

During the iterative process analytic solutions are used to compute estimates of $\boldsymbol{A}$ (where $\boldsymbol{S}_2$ or $\boldsymbol{S}_3$ is assumed to be known) and $\boldsymbol{S}_2$ or $\boldsymbol{S}_3$ (where $\boldsymbol{A}$ and $\boldsymbol{S}_1$ are assumed to be known):

$$\begin{cases} \hat{A}^i = X\hat{S}^T\left(\hat{S}\hat{S}^t + \lambda_A I\right)^{-1} \\ \widehat{S}_k^i = \left(\hat{A}_k^t\hat{A}_k + \lambda_{S_k} I\right)^{-1}(\hat{A}_k^t X - \hat{A}_l^t\hat{A}_k\hat{S}_l) \end{cases} \tag{36}$$

In contrast, it derives from the non-differentiability of the penalty function $\lambda_1\|\boldsymbol{S}_1\|_1$ in the objective function $J(\boldsymbol{S_1}) = \|\boldsymbol{X} - \boldsymbol{A}_k\boldsymbol{S}_k - \boldsymbol{A}_1\boldsymbol{S}_1\|_2^2 + \lambda_1\|\boldsymbol{S}_1\|_1$ deriving from Eq.(33), there are no closed-form solutions for $J(\boldsymbol{S_1})$ that can be used in the update rule for $\boldsymbol{S}_1$. Thus, we need to use an optimization scheme for this step. The $\boldsymbol{L}_1$ norm regularized least squares LASSO [20] that seeks the minimizer of $J(\boldsymbol{S_1})$ is chosen in this study because it provides the best performance in the sense of the sparsity/measurement tradeoff.

8.3 JMAP SPARSE : Sparsity prior for $\boldsymbol{S_2}$ and Gaussian for $\boldsymbol{S_3}$

This last case is quite similar of the one examined in Section 8.2 but here, since it is applied a sparsity prior for $\boldsymbol{S}_2$ and a Gaussian one for $\boldsymbol{S}_3$, and the subscripts 1 and k are replaced with 2 and 3 respectively in Eqs.(33), (34) and (35).

Again, due to the non-differentiability of the penalty function $\lambda_2\|\boldsymbol{S}_2\|_1$ in the objective function function $J(\boldsymbol{S_2}) = \|\boldsymbol{X} - \boldsymbol{A}_2\boldsymbol{S}_2 - \boldsymbol{A}_3\boldsymbol{S}_3\|_2^2 + \lambda_2\|\boldsymbol{S}_2\|_1$, there are no closed-form solutions for $J(\boldsymbol{S_2})$that can be used in the update rule for $\boldsymbol{S}_2$ Thus, we need to use an optimization scheme for this step done with regularized least squares LASSO [20].

9 SEPARATION RESULTS

The Bayesian source separation approach presented in Section 8 is applied here on the data recorded during the experiment described in Section 5. In the first part, it is examined the separation results when the mixtures are performed artificially (see Section 6) and in the second part when they are measured directly with the array of microphones (see Section 5). We consider for both kind of mixtures that the priors for the mixing matrix (Eq.(27)) and the likelihood (Eq.(29)) are Gaussian. The cases 1 to 3 of source priors defined in Section 7.1 will be studied for the observations mixed artificially, while only cases 2 and 3 will be considered for the mixtures directly measured.

9.1 Separation results of real data mixed artificially

The PSD observations pairwise mixed artificially (lower plots in Fig.5) are unmixed in Fig.6, based on Eqs.(30), (31) and (32), with $\lambda_A = 800$, $\lambda_{S_k} = 0.2$ and $\lambda_{S_l} = 0.001$ (the subscripts k, l are defined in Eq.(24)). The background noise remains high. Nevertheless, the frequency radiation of the tonal source is well retrieved in the PSD of $\boldsymbol{S}_1$ when it is mixed with $\boldsymbol{S}_2$ or $\boldsymbol{S}_3$. In contrast, the separation result concerning the mixture ($\boldsymbol{S}_2 + \boldsymbol{S}_3$) is not totally well done.

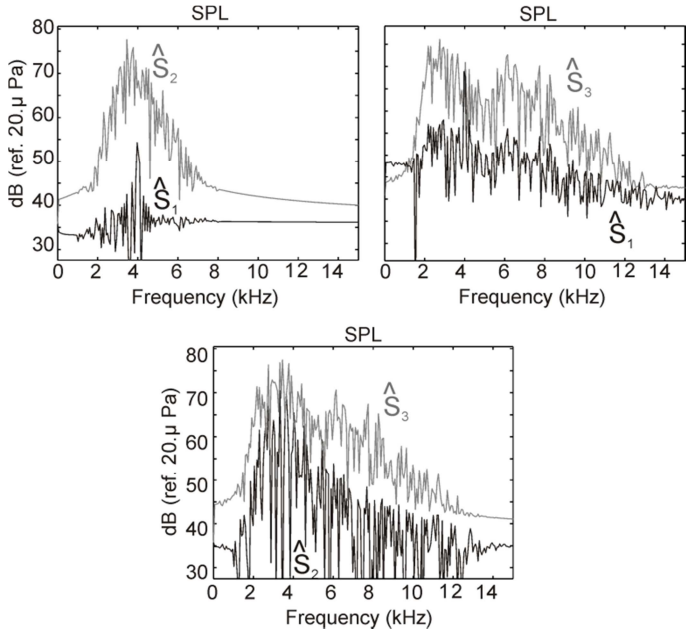

Fig.6. Case of observations mixed artificially - Unmixed PSDs ($\boldsymbol{S}_1 + \boldsymbol{S}_2$), ($\boldsymbol{S}_1 + \boldsymbol{S}_3$) and ($\boldsymbol{S}_2 + \boldsymbol{S}_3$) using Gaussian priors for $\boldsymbol{S}_1$, $\boldsymbol{S}_2$ and $\boldsymbol{S}_3$.

It is examined the unmixed PSDs of ($\boldsymbol{S}_1 + \boldsymbol{S}_2$) and ($\boldsymbol{S}_1 + \boldsymbol{S}_3$) when a sparsity prior is affected to $\boldsymbol{S}_1$ and Gaussian one to $\boldsymbol{S}_2$ or $\boldsymbol{S}_3$ (here $\lambda_A = 800$, $\lambda_{S_k} = 0.3$ and $\lambda_{S_l} = 1.65$, the subscripts $k = 1$, $l = 2$ *or* 3). The interest of sparsity prior clearly appears on the separation results shown in Fig.7. Only a peak at 4 kHz is found in the estimate $\widehat{\boldsymbol{S}}_1$ of the PSD tonal source $\boldsymbol{S}_1$. Moreover, the shapes of the original source spectra $\boldsymbol{S}_2$ and $\boldsymbol{S}_3$ are correctly restored in $\widehat{\boldsymbol{S}}_2$ and $\widehat{\boldsymbol{S}}_3$ respectively.

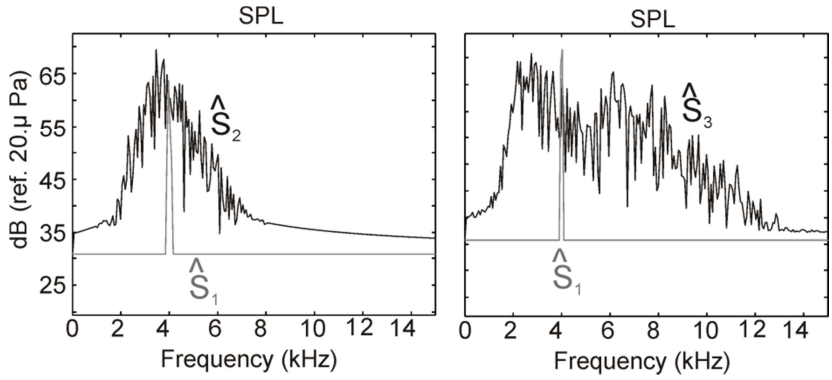

Fig.7. Case of observations mixed artificially - Unmixed PSDs ($\boldsymbol{S}_1$ + $\boldsymbol{S}_2$) and ($\boldsymbol{S}_1$ + $\boldsymbol{S}_3$) using Laplace prior for $\boldsymbol{S}_1$ and Gaussian prior for $\boldsymbol{S}_2$ and $\boldsymbol{S}_3$.

The unmixed PSDs of ($\boldsymbol{S}_2$ + $\boldsymbol{S}_3$) (with $\lambda_A = 800$, $\lambda_{S_k} = 0.3$ and $\lambda_{S_l} = 1.65$, k=2 and l=3) with a sparsity prior affected to $\boldsymbol{S}_2$ and a Gaussian to $\boldsymbol{S}_3$ show again, the interest of sparsity prior in Fig.8. The frequency supports where both sources $\widehat{\boldsymbol{S}}_2$ and $\widehat{\boldsymbol{S}}_3$ are emitting are well restored and their original PSDs shapes too.

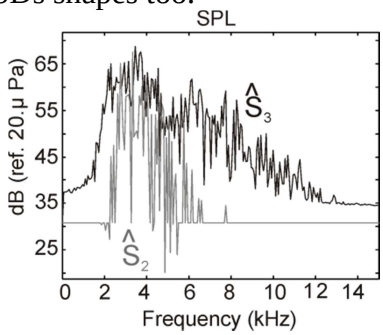

Fig.8. Case of observations mixed artificially - Unmixed PSD ($\boldsymbol{S}_2$ + $\boldsymbol{S}_3$) using Laplace prior for $\boldsymbol{S}_2$ and Gaussian Prior for $\boldsymbol{S}_3$.

9.2 Experimental results

The Bayesian source separation are applied in this section to the mixtures ($\boldsymbol{S}_1$ + $\boldsymbol{S}_2$), ($\boldsymbol{S}_1$ + $\boldsymbol{S}_3$) and ($\boldsymbol{S}_2$+ $\boldsymbol{S}_3$) measured during the experiment described in Section 5. The reference signals Ref_1, Ref_2, and Ref_3 shown in Fig.9 (upper plots) considered here are not filtered compared to the case studied with the artificial mixtures (see Fig.4).The consequence is that the histogram of $\boldsymbol{S}_1$ seems to be characterized by a Gaussian distribution and this remark can be applied for the histograms of $\boldsymbol{S}_2$ and $\boldsymbol{S}_3$ (Fig.9) center graphs). The scatter plots of the joint distributions (Fig.9 lower graphs) present a distribution of two independent Gaussian signals for ($\boldsymbol{S}_1$, $\boldsymbol{S}_2$) , ($\boldsymbol{S}_1$, $\boldsymbol{S}_3$) and ($\boldsymbol{S}_2$, $\boldsymbol{S}_3$).

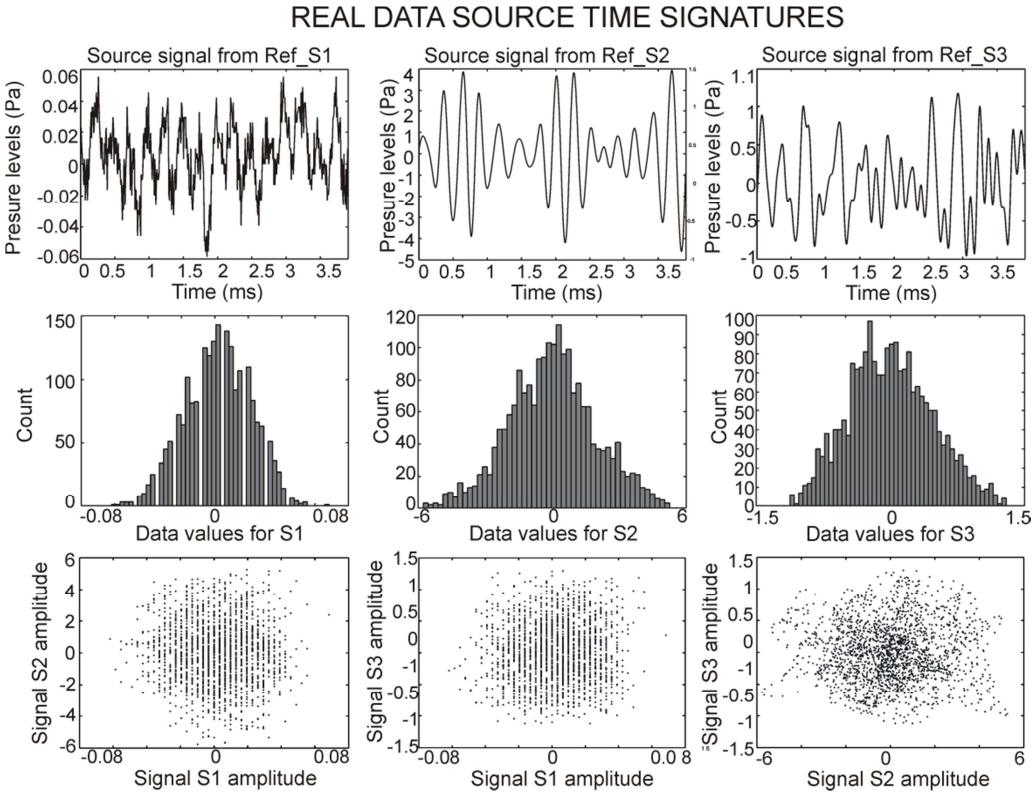

Fig.9. Real data - Primary sources measured by Ref_1, Ref_2, and Ref_3 microphones (upper); Histograms of the primary sources (centre); Joint distributions of the primary sources (lower)

It is presented in the upper plots of Fig.10 the spectra of the reference source signals. As it was foreseeable, the PSD of the sinus signal is here noisier than its filtered version presented in the upper plots in Fig.5. The PSDs of ($\boldsymbol{S}_1$, $\boldsymbol{S}_2$) , ($\boldsymbol{S}_1$, $\boldsymbol{S}_3$) and ($\boldsymbol{S}_2$, $\boldsymbol{S}_3$) measured with microphone 1 of the array are superimposed from left to right in Fig.10 and the mixtures of the PSDs of ($\boldsymbol{S}_1 + \boldsymbol{S}_2$), ($\boldsymbol{S}_1 + \boldsymbol{S}_3$) and ($\boldsymbol{S}_2 + \boldsymbol{S}_3$) presented in the lower graphs.

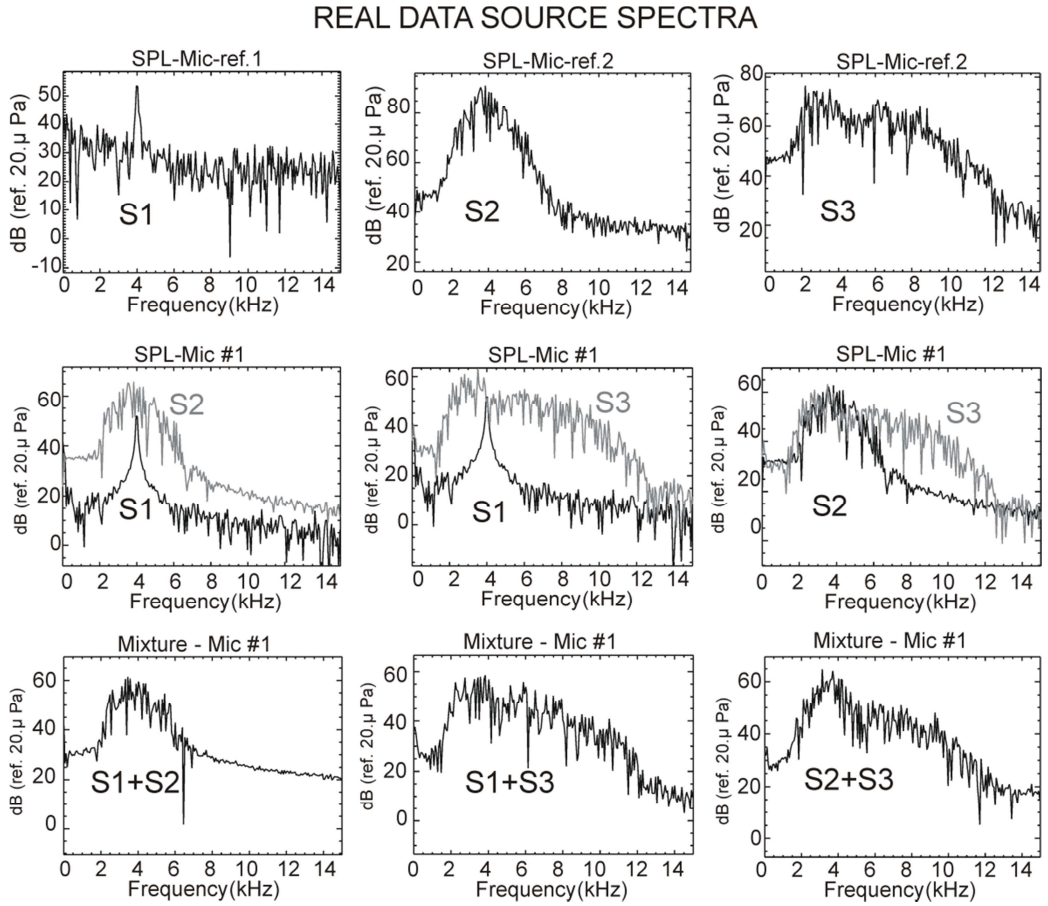

Fig.10. Real data - PSDs of the reference source signals measured with a microphone of the array (upper) -PSDs of reference source signals superimposed pairwise (centre) - PSDs of the mixture when the loadspeakers where pairwise active (lower).

The separation results obtained with real data mixed pairwise artificially, presented in Section 9.1, have clearly demonstrated the interest to use sparsity priors when we are in presence of a primary source with an acoustic emission in a frequency band much narrow than those of another primary source. It is why, only the case 2 of Section 7.1 will be considered here. The priors for the mixing matrix (Eq.(27)) and the likelihood (Eq.(29)) are again chosen Gaussian for the reason already explained in Sections 7.1. The unmixed PSDs of ($\boldsymbol{S}_1 + \boldsymbol{S}_2$) and ($\boldsymbol{S}_1 + \boldsymbol{S}_3$) and ($\boldsymbol{S}_2 + \boldsymbol{S}_3$) presented in Fig. 11, show that the Bayesian source separation approach is quite relevant in the acoustic signals demixing.

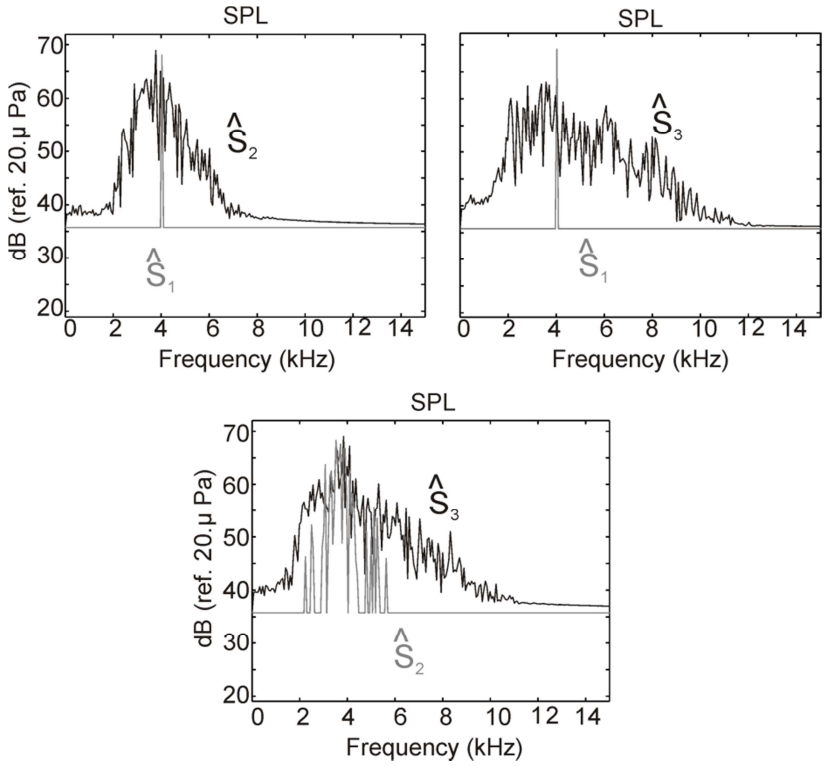

Fig.11. Real data - Unmixed PSDs ($\boldsymbol{S}_1$ + $\boldsymbol{S}_2$), ($\boldsymbol{S}_1$ + $\boldsymbol{S}_3$) with Laplace prior for $\boldsymbol{S}_1$ and Gaussian prior for $\boldsymbol{S}_2$ and $\boldsymbol{S}_3$; Unmixed PSD ($\boldsymbol{S}_2$+ $\boldsymbol{S}_3$) with Laplace prior for $\boldsymbol{S}_2$ and Gaussian prior for $\boldsymbol{S}_3$.

10 CONCLUSIONS

In this paper, we considered the source separation problem in a Bayesian framework. We compared the separation results involving a tonal source, a broadband source and a wideband one mixed pairwise, based on JMAP. For the broadband signal, we use a Gaussian prior and for very narrow or tonal we use a Laplace prior. For each case, first the expression of the joint posterior law $p(\boldsymbol{A},\boldsymbol{S}|\boldsymbol{X},\boldsymbol{\theta})$ is obtained and then optimized via an alternating optimization algorithm. The main conclusion are:

- first, the Bayesian approach could be used efficiently on simulated and real data,
- second, it that using appropriate priors (Gaussian for the broadband and Laplace for the narrowband or tonal) greatly improve the separation results.

REFERENCES

[1] H. Ran and D. Mavris, “Preliminary design of a 2d supersonic inlet to maximize total pressure recovery,” in AIAA 5th Aviation, Technology, Integration, and Operations Conference (ATIO), Arlingto, VA, 2005.

[2] J. M. Brookfield and I. A. Waitz, “Trailing-edge blowing for reduction for reduction of turbomachinery fan noise,” Journal of Propulsion and Power, vol. 16, no. 1, pp. 57–64, January-February 2000.

[3] B. D. Mugridge, “The measurement of spinning acoustic modes generated in an axial flow fan,” J. Sound Vib., vol. 10, no. 2, pp. 227–246, January-February 1969.

[4] S. Martens, “Jet noise reduction technology development at GE aircraft engines,” in ICAS 2002 CONGRESS, 2002.

[5] Y. Li, M. Smith, and X. Zhang, “Measurement and control of aircraft landing gear broadband noise,” in Aerospace Science and Technology, 2012.
[6] Y. Tani, Y. Matsuda, A. Doi, Y. Yamashita, S. Aso, and T. Ito, “Experimental study of the morphing flap as a low noise high lift device for aircraft wing,” in 28th International Congress Of The Aeronautical Sciences, 2012.
[7] C. K. W. Tam, Computational Aeroacoustics A WAVE NUMBER APPROACH. Cambridge University Press, 2012.
[8] I. L. Griffon, “Aircraft noise modelling and assessment in the IESTA program with focus on engine noise,” in The 22nd International Congress on Sound and Vibration, Florence (Italy), 2015.
[9] D. Blacodon and G. Elias, “Level estimation of extended acoustic sources using a parametric method,” J. of Aircraft, vol. 41, no. 6, pp. 1360–1369, June. 2004.
[10] D. Blacodon, “Spectral estimation method for noisy data using a noise reference,” Applied Acoustics, vol. 72, no. 1, pp. 11–21, January 2011.
[11] N. Chu, J. Picheral, and A. Mohammad-Djafari, “A robust super-resolution approach with sparsity constraint in acoustic imaging,” Applied Acoustics, vol. 76, pp. 197–208, February 2014.
[12] P. Comon and C. Jutten, Handbook of Blind Source Separation Independent Component Analysis and Applications. Academic Press is an imprint of Elsevier, 2010.
[13] C. Févotte and S. J. Godsill, “A Bayesian approach for blind separation of sparse sources,” IEEE Transactions On Audio, Speech, And Language Processing, vol. 14, no. 6, pp. 2174–2188, Nov. 2006.
[14] H. Snoussi and A. Mohammad-Djafari, “A mean field approximation approach to blind source separation with Lp priors,” in Signal Processing Conference 2005 13th European, 2005.
[15] A. Belouchrani, K. Abed-Meraim, J.-F. Cardoso, and E. Moulines, “A blind source separation technique using second-order statistics,” IEEE Transactions On Signal Processing, vol. 45, no. 2, pp. 2174–2188, Feb. 1997.
[16] M. S. Pedersen, J. Larsen, U. Kjems, and L. C. Parra, A Survey of Convolutive Blind Source Separation Methods. Springer Press, 2007.
[17] P. Comon, “Independent component analysis a new concept?” Signal Processing, vol. 36, pp. 287–314, April 1994.
[18] S. Kullback, Information theory and statistics. Dover Publication, 1959.
[19] A. Mohammad-Djafari, “Bayesian blind deconvolution of images comparing JMAP, EM and BVA with a student-t a priori model,” in Scientific Cooperations International Workshops on Electrical and Computer Engineering Subfields, Koç University, Istanbul/Turkey, 2014.
[20] R. Tibshirani, “Regression Shrinkage and Selection via the Lasso,” Journal of the Royal Statistical Society: Series B, vol. 58, no. 1, pp. 267–288, 1996.